ACTA METALLURGICA SLOVACA
2021, VOL. 27, NO. 3, 122-126

RESEARCH PAPER

HEAT TREATMENT EFFECT ON MARAGING STEEL MANUFACTURED BY LASER POWDER BED FUSION TECHNOLOGY: MICROSTRUCTURE AND MECHANICAL PROPERTIES

Giulia Stornelli[1], Damiano Gaggia[2], Marco Rallini[3], Andrea Di Schino[4]

[1] Università di Roma Tor Vergata, Dipartimento di Ingegneria Industriale, Roma, Italy
[2] Green Tales Srl, Terni, Italy
[3] Università degli Studi di Perugia, Dipartimento di Ingegneria Civile e Ambientale, Perugia, Italy
[4] Università degli Studi di Perugia, Dipartimento di Ingegneria, Perugia, Italy

* Corresponding author: giulia.stornelli@students.uniroma2.eu, Dipartimento di Ingegneria Industriale, Università di Roma Tor Vergata, Via Cracovia, 50, 00133, Roma, Italy

Received: 19.05.2021
Accepted: 19.06.2021

ABSTRACT

Laser Powder Bed Fusion (L-PBF) is a widespread additive manufacturing technology in industrial applications, for metal components manufacturing. Maraging steel is a special class of Fe-Ni alloys, typically used in the aerospace and tooling sectors due to their good combination of mechanical strength and toughness. This work analyses the heat treatment effect on the microstructure and hardness value of 300-grade maraging steel manufactured by the L-PBF process. The considered heat treatment consists of a solution annealing treatment followed by quenching and ageing hardening treatment. The effect of ageing temperature is reported, in a wide temperature range. Results show that solution annealing treatment fully dissolves the solidification structure caused by the L-PBF process. Moreover, the ageing hardening treatment has a significant impact on the hardness, hence on strength, of L-PBF maraging steel. The optimal ageing conditions for the L-PBF maraging steel are identified and reported: in particular, results show that the hardness of 583 HV is achieved following ageing treatment at 490 °C for 6 hours. A higher treatment temperature leads to over-ageing resulting in a decrease of hardness. Conversely, an excessive ageing time does not seem to affect the hardness value, for the ageing temperature of 490 °C.

Keywords: Maraging steel; Additive manufacturing; Laser Powder Bed Fusion; Ageing hardening treatment;

INTRODUCTION

Maraging steels are a special class of ultra-high-strength Fe-Ni alloys [1] mainly used in aircraft and aerospace applications and for precision gears and moulds [1-4]. Maraging steels are highly alloyed steels (primarily with Ni, Co, Mo, Ti and Al [5]) whit a low carbon content [6, 7] which exhibit excellent mechanical properties such as high strength and hardness and good toughness and ductility [3]. Maraging refers to a martensitic matrix hardened by second phases precipitated during an ageing treatment [8]. The martensite microstructure is easily obtained in this steel owing to the high Ni content [9] and is formed by cooling at moderate rates from a solid solution of γ-Fe containing Ni [1]. The structure thus obtained is a soft-martensite [3] thanks to the low carbon content, but heavily dislocated [9]. The main difference concerning other steels is to be found in the fact that maraging steels are not strengthened by carbon content [10-16] and that the main strengthening effect is related to intermetallic compounds precipitation [10]. During the ageing treatment, typically in 400°C-700°C range temperature [17] the precipitation mechanism of nano-sized and homogeneous dispersed intermetallic compounds (such as Fe_2Mo, NiAl, $Ni_3(Ti, Al, Mo)$, Ni(Al, Fe), etc.) is promoted [4, 18], enhancing the microhardness and strength by dislocation motion inhibition [3, 19]. Therefore, the ageing hardening treatment is the key issue to be analysed aimed to guarantee strength and toughness combination in the maraging steels [20].

Conventionally, the maraging steels are produced by casting process with subsequent deformation process, solution annealing heat treatment, quenching, machining and final ageing heat treatment [21].

For several years, following the increasing adoption of additive manufacturing (AM) technologies, the Fe-based alloys powders began to be used for the production of engineering parts [10, 22-24]. Currently, the most widespread AM process for the metal in industrial applications is laser powder-bed fusion technology (L-PBF) [8, 25-27]. The L-PBF technology uses the laser source as an energy source to melt the metal powders and the components are built, layer by layer [28-30], directly from Computer-Aided Design (CAD) models [24,31].

To date, there are numerous studies focused on the possibility to produce maraging steel components through L-PBF technology (e.g., [32-34]). Its low carbon content and good ductility help to prevent crack formation during rapid cooling [18] typical of AM technologies and no special care are needed to avoid carbides or carbon segregation related problems [34]. Moreover, due to high cost, the maraging steels are often used in the sector, such as aerospace or tool-manufacturing industries, which require the combination of complex geometries

and excellent mechanical properties that can be well fulfilled by the L-PBF process [21, 35-38].
The scientific research about the production of maraging steel by L-PBF technology has been focused on the optimization of the process parameters and the condition of solution annealing and ageing heat treatments [39]. Many efforts have shown that an appropriate choice of the scanning strategy and the operating parameters of the laser source, allow producing the maraging steel compounds with high relative density and high performance (e.g., [11, 19, 40, 41]).
For example, Casilino et al. [42] investigated the effect of the variation of the laser process parameters on the densification of 18Ni 300-grade maraging steel. The authors found that a relative density of higher than 99% is achieved by using a laser power above 90W and a scanning speed less than 220 mm/s. Mutua et al. [11] defined a large operative window of the process parameters in which, for 300-grade steels, it's possible to achieve a relative density above 99%. While all the aforementioned studies were on 300-grade, Brookes [43] has examined the influence of energy density on samples density, hardness and tensile properties of 200-grade maraging steel.
In the studies just mentioned, the microstructure obtained by the L-PBF process of 300-grade maraging steel returns to be very fine and cellular type, given the rapid solidification rates involved in the additive manufacturing processes [4, 11, 44]. Song et al. [6] and Conde et al. [8] investigated the effect of various solution annealing and ageing heat treatment conditions on the mechanical behaviour of maraging steel by L-PBF and found that the solution annealing treatment leads to a decrease in strength compared with as-built samples. The subsequent precipitation of intermetallic compounds following the ageing treatment increases the yield strength, ultimate tensile strength and hardness values.
This paper aims to analyze, with a systematic approach, the effect of a temperature-time combination of ageing heat treatment on 18Ni 300-grade maraging steel based on the L-PBF technology. The effect of ageing heat treatment is reported in terms of microstructure and hardness value. In particular, the mechanical behaviour of maraging steel after ageing treatment was compared with as-built and solution annealed sample.

MATERIAL AND METHODS

In this study, 300-grade maraging steel powder is used. The powder was produced by gas atomization and the nominal chemical composition (wt.%) is reported in **Table 1**.

Table 1 Nominal chemical composition of 300-grade maraging steel powders (wt%)

Element	Max.	Min.
Fe	To balance	
Ni	17.00	19.00
Co	8.50	9.50
Mo	4.50	5.20
Ti	0.60	0.80
Al	0.05	0.15
Cr	0.50	-
Cu	0.50	-
C	0.03	-
Mn	0.10	-
Si	0.10	-
P	0.01	-
S	0.01	-

The particle morphology was characterized by a high-resolution scanning electron microscope (FE-SEM Zeiss, Gemini Supra 25). As shown in **Fig. 1** the morphology of the powders was generally spherical and some particles have satellites. Moreover, a fraction of elliptic shape particles can be observed.

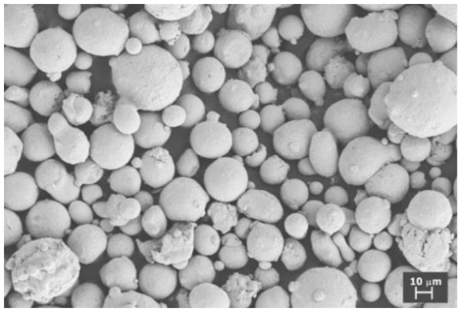

Fig. 1 Powders morphology of 300-grade maraging steel, SEM image

The powders were processed through a system with L-PBF technology (Eos M290) to produce test samples. The machine used for manufacturing is equipped with a 400 W precision optics F-theta lens Yb fibre laser with a nominal diameter of 100 µm and the platform temperature was kept at 40 °C. The process was carried out under nitrogen atmosphere and the parameters of the melting process used are as follows: laser power of 400 W, scanning speed up to 0.7 ms^{-1}, layer thickness 50 µm.
Following the manufacturing process of the maraging steel samples, a Solution Annealing Treatment and Quenching (SAT + Q) was carried out according to the heating profile as reported in **Fig. 2**.

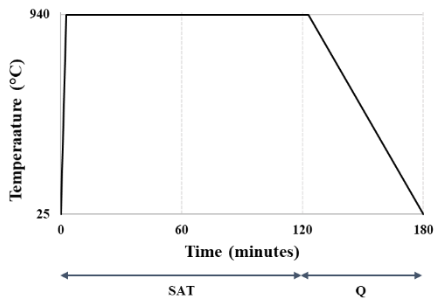

Fig. 2 SAT + Q heat profile

The time-temperature condition of SAT + Q has been performed to guarantee a high degree of homogenization of the composition and, in particular, to dissolve the cellular and columnar microstructure and micro-segregation, typically induced by the additive manufacturing process [7, 8].
Subsequently, to study the effect of ageing hardening treatment (AHT), various combinations of time-temperature were investigated. In particular, ageing heat treatments were carried out at a temperature between 450 °C and 550 °C and in the 6-24 hours range time.
A summary of heat treatment parameters is reported in Table 2 (SAT + Q and AHT).
The test samples were machined along a plane parallel to the build direction (BD), polished and etched with a solution of 2% Nital. An optical microscope (OM) (Eclipse LV150NL, Nikon) and a high-resolution scanning electron microscope (SEM) (FE-SEM Zeiss, Gemini Supra 25) was used to investigate the microstructure of 300-grade maraging steel by L-PBF process. In particular, the microstructural analysis was carried out for

each state of the steel: as-built sample, after solution annealing treatment and quenching, after the various time-temperature combination of the ageing treatment.
Moreover, for the same samples, the hardness value (HV10) were measured to evaluate the best ageing condition, in term of strengthening.

Table 2 Heat treatments scheme carried out on 300-grade maraging steel based on L-PBF process

Experiment No.	SAT + Q			AHT	
	Temperature (°C)	SAT holding time (hours)	Cooling rate (°C/minutes)	Temperature (°C)	Ageing time (hours)
1	940	2	16	450	6
2	940	2	16	470	6
3	940	2	16	490	6
4	940	2	16	490	10
5	940	2	16	490	24
6	940	2	16	510	6
7	940	2	16	530	6
8	940	2	16	550	6

RESULTS AND DISCUSSION

Effect of solution annealing treatment and quenching on L-PBF maraging steel.

The OM image in **Fig. 3** shows the low-magnification microstructure of the as-built sample of 300-grade maraging steel in the vertical plane (parallel to build direction). Laser tracks are visible after the etching of the sample (red dotted line). In **Fig. 4**, other details of microstructure are shown in the high magnification SEM image. The solidification structure on the melt pool (delimitate by red dotted line) is composed of a mixture of columnar (black arrows) and cellular (red arrows) morphology, typical of steel produced by AM technology. However, the cellular structure is predominant due to the fast cooling rate within the melt pool during the L-PBF process [45].
The value of HV10 of the as-built sample is 384 HV.
Fig. 5 and **Fig. 6** show, respectively, the optical and SEM images of the maraging steel after the SAT + Q heat treatment. The microstructure changes visibly compared to the as-built sample: the laser traces disappear completely and the cellular and columnar structure have been replaced by lath martensite. The condition of SAT + Q tested in this work lead to microstructure with large lath.
After SAT + Q heat treatment the hardness of the sample is 312 HV.

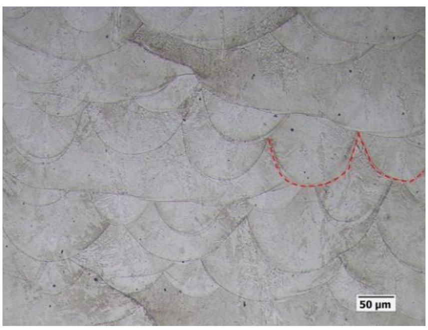

Fig. 3 Optical image of the as-built sample of 300-grade maraging steel along the built direction. The red dotted line delimitates the boundaries of the melt pool

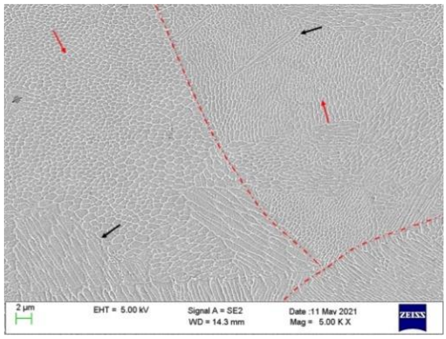

Fig. 4 SEM image of the as-built sample. Details of solidification structure with different morphology: cellular (red arrows) and columnar (black arrows)

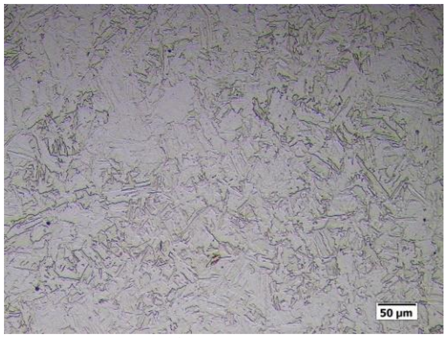

Fig. 5 Optical image of 300-grade maraging steel-based L-PBF process and after SAT + Q heat treatment

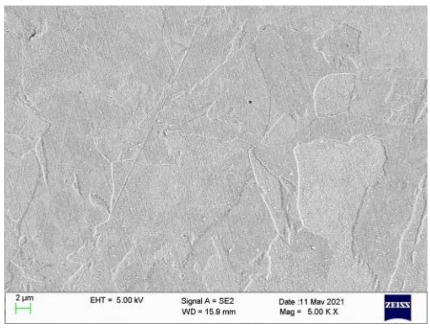

Fig. 6 SEM image of 300-grade maraging steel-based L-PBF process and after SAT + Q heat treatment

Ageing hardening treatment effect on L-PBF maraging steel

Various conditions of ageing hardening treatment were carried out on the sample, in terms of time and temperature, after the solution annealing treatment and quenching. In particular, six treatment temperature were investigated in the range from 450 °C to 530 °C, with an ageing time of 6 hours. **Fig. 7** shows the effect of ageing treatment on the hardness value of 300-grade maraging steel by the L-PBF process. The best condition of ageing treatment corresponds to a temperature of 490 °C and 6 hours of ageing time. The hardness value worsens drastically with the increasing temperature. As it is known from the literature, with a high treatment temperature or for a long ageing time, the physical phenomena activated by this excessive treatment condition lead to degradation of the strength of the maraging steel [4]. Over 490°C, the over-ageing occurs, the intermetallic compounds coarsened and the reconversion of the metastable martensite into austenite being [46]. About that, for an ageing treatment at 550 °C for 6 hours, the hardness decreases by about 50 HV, going from 583 HV for a temperature of 490°C, to 532 HV at 550 °C. **Fig. 8** and **Fig. 9** show, respectively, the SEM images relating to the best (490 °C, 6 hours) and the worst (550°C, 6 hours) ageing treatment conditions, in terms of hardness.

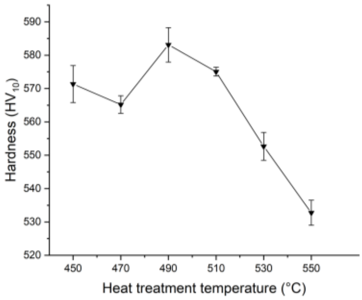

Fig. 7 Effect of heat treatment temperature on hardness (HV_{10}) of maraging steel produced by L-PBF process. Ageing time: 6 hours

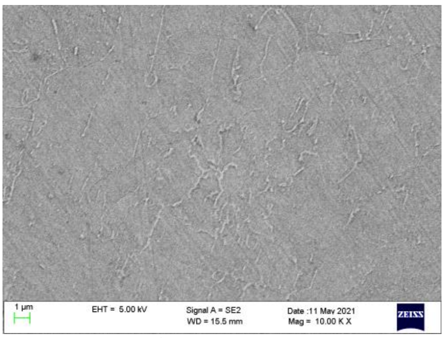

Fig. 8 SEM image of 300-grade maraging steel produced by L-PBF technology referred to the best AHT (490 °C, 6 hours) condition, in terms of hardness value

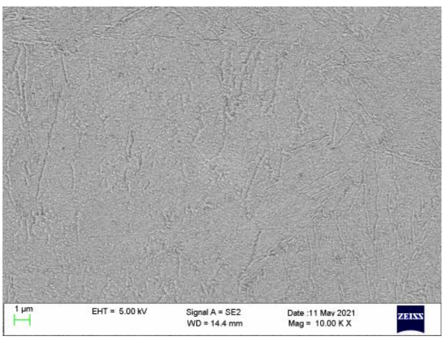

Fig. 9 SEM image of 300-grade maraging steel produced by L-PBF technology referred to the worst AHT (550°C, 6 hours) condition, in terms of hardness value

Moreover, the effect of ageing time on hardness value was investigated for the best treatment temperature (490 °C). As shown in **Fig. 10**, the influence of time on the over-ageing phenomenon is not as relevant as it is for the influence of treatment temperature. Conversely, the hardness values seem not to be affected by the time effect, after 24 hours of treatment the hardness is 590 HV against 583 HV for 6 hours of treatment.

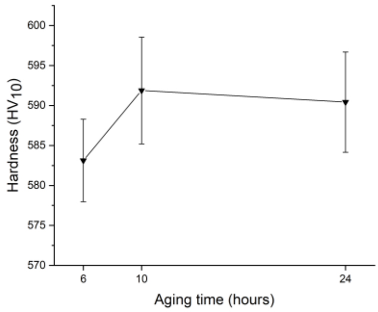

Fig. 10 Effect of ageing time on hardness (HV_{10}) of maraging steel produced by L-PBF process. Heat treatment temperature: 490 °C

CONCLUSION

An experimental campaign was conducted to investigate the heat treatment effect on microstructure and hardness value of 300-grade maraging steel manufactured by the L-PBF process. In particular, the behaviour of the maraging steel after solution annealing at 940 °C for 2 hours and quenching and after ageing hardening treatment is reported. The ageing treatment was carried out for different time-temperature combinations: treatment temperature from 430 °C to 550 °C and ageing time from 6 to 24 hours were considered. The main conclusions can be summarized as follow:

- the microstructure of the maraging steel after the L-PBF process turns out to be mainly of cellular type, with some areas characterized by columnar structure. After the solution annealing at 940 °C for 2 hours and quenching, the solidification structure and the boundaries of laser traces were completely replaced by lath martensite microstructure. The hardness passes from 384 HV for the as-built sample to 312 HV after solution annealing treatment and quenching.
- Ageing hardening treatment is crucial to improve the properties of maraging steel produced with technology. A hardness value of 583 HV was measured for a treatment temperature of 490 °C and an ageing time of 6 hours. For high ageing temperature, there are physical phenomena such as coarsened of intermetallic compounds and/or reversed austenite which decrease the strength of the maraging steel. About that, a decrease of hardness occurred for temperature above 490 °C; 530 HV is the hardness value found for an ageing treatment at 550 °C for 6 hours.
- The ageing time effect was analysed for the best ageing treatment temperature. The hardness of maraging steel produced with L-PBF technology, aged at 490 °C, does not seem to depend on time. The difference in hardness after 6 hours of treatment and 24 hours of treatment turns out to be less than 10 HV.

REFERENCES

1. R. Casati, J. N. Lemke, A. Tuissi, M. Vedani: Metals, 6(9), 2016, 218. https://doi.org/10.3390/met6090218.
2. E. A. Jägle, Z. Sheng, P. Kürnsteiner, S. Ocylok, A. Weisheit, D. Raabe: Materials, 10(1), 2017, 8. https://doi.org/10.3390/ma10010008.
3. B. Mooney, K. I. Kourousis: Metals, 10(9), 2020, 1273. https://doi.org/10.3390/met10091273.
4. Y. Bai, D. Wang, Y. Yang, H. Wang: Materials Science and Engineering: A, 760, 2019, 105–117. https://doi.org/10.1016/j.msea.2019.05.115.
5. L. Kučerová, I. Zetková, A. Jandová, M. Bystrianský: Materials Science and Engineering: A, 750, 2019, 70-80. https://doi.org/10.1016/j.msea.2019.02.041.
6. J. Song et al.: Optics and Laser Technology, 120, 2019, 105725. https://doi.org/10.1016/j.optlastec.2019.105725.
7. A. Bagchi, D. K. Gope, S. Chattopadhyaya, G. Wuriti: Materials Today Proceedings, 27, 2019, 2303–2307. https://doi.org/10.1016/j.matpr.2019.09.117.
8. F. F. Conde et al.: Materials Science and Engineering: A, 758, 2019, 192–201. https://doi.org/10.1016/j.msea.2019.03.129.
9. W. Sha, G. Zhanli: *Maraging steels: Modelling of microstructure, properties and applications*. Cambridge (UK), Woodhead Publishing, 2009.
10. X. Xu, S. Ganguly, J. Ding, S. Guo, S. Williams, F. Martina: Materials Characterization, 143, 2018, 152–162. https://doi.org/10.1016/j.matchar.2017.12.002.
11. J. Mutua, S. Nakata, T. Onda, Z. C. Chen: Materials and Design, 139, 2018, 486–497. https://doi.org/10.1016/j.matdes.2017.11.042.
12. A. Di Schino: Metalurgija, 56(3-4), 2017, 349-352.
13. A. Di Schino, L. Alleva, M. Guagnelli: Materials Science Forum, 715-716, 2012, 860-865. https://doi.org/10.4028/www.scientific.net/MSF.715-716.860.
14. G. Stornelli et al: Materials Science Forum, 1016, 2021, 1392–1397. https://doi.org/10.4028/www.scientific.net/MSF.1016.1392.
15. A. Di Schino, P.E. Di Nunzio: Acta Metall. Slovaca, 23, 2017, 62-71. https://doi.org/10.12776/ams.v23i1.852.
16. A. Di Schino, P. Di Nunzio, G.L. Turconi: Mater. Sci. Forum, 558-559, 2007, 1435-1441. https://doi.10.4028/www.scientific.net/MSF.558-559.1435.
17. J. M. Pardal, S. S. M. Tavares, M. P. Cindra Fonseca, H. F. G. Abreu, J. J. M. Silva: Journal of Materials Science, 41(8), 2006, 2301–2307. https://doi.org/10.1007/s10853-006-7170-y.
18. C. Tan, K. Zhou, M. Kuang, W. Ma, T. Kuang: Science and Technology of Advanced Materials, 19(1), 2018, 746–758. https://doi.org/10.1080/14686996.2018.1527645.
19. Y. Bai, Y. Yang, D. Wang, M. Zhang, Materials Science and Engineering A, 703, 2017, 116–123. https://doi.org/10.1016/j.msea.2017.06.033.
20. F. F. Conde, J. D. Escobar, J. P. Oliveira, A. L. Jardini, W. W. Bose Filho, J. A. Avila: Additive Manufacturing, 29, 2019, 100804. https://doi.org/10.1016/j.addma.2019.100804.
21. E. A. Jägle, P. P. Choi, J. Van Humbeeck, D. Raabe: Journal of Materials Research, 29(17), 2014, 2072-2079. https://doi.org/10.1557/jmr.2014.204.
22. G. Stornelli et al.: La Metallurgia Italiana, 113, 2021, 50-63.
23. R. Bidulský et al.: Materials, 13(5), 2020, 3328. https://doi.org/10.3390/ma13153328.
24. G. Stornelli et al.: Materials, 14(6), 2021, 1489. https://doi.org/10.3390/ma14061489.
25. A. Di Schino; Metals, 10(3), 2020, 327. https://doi.org/10.3390/met10030327.
26. C. Zitelli, P. Folgarait and A. Di Schino: Metals, 9(7), 2019, 731. https://doi.org/10.3390/met9070731.
27. M. Ridolfi, P. Folgarait and A. Di Schino: Materials, 13(6), 2020, 1424. https://doi.org/10.3390/ma13061424.
28. J. Savolainen, M. Collan: Additive Manufacturing, 32, 2020, 101070. https://doi.org/10.1016/j.addma.2020.101070.
29. M.R. Ridolfi, P. Folgarait, A. Di Schino: Acta Metallurgica Slovaca, 26, 2020, 7-10. https://doi.org/10.36547/ams.26.1.525.
30. D. Manfredi, R. Bidulský: Acta Metallurgica Slovaca, 23, 2017, 276-282. https://doi.org/10.12776/ams.v23i3.988.
31. B. Vicenzi, K. Boz, L. Aboussouan: Acta Metallurgica Slovaca, 26, 2020, 144-160. https://doi.org/10.36547/ams.26.4.656.
32. A. Fortunato, A. Lulaj, S. Melkote, E. Liverani, A. Ascari, D. Umbrello: International Journal of Advanced Manufacturing Technology, 94(5-8), 2018, 1895–1902. https://doi.org/10.1007/s00170-017-0922-9.
33. E. Yasa, K. Kempen, J. P. Kruth: *Solid freeform fabrication symposium proceedings*, 2010, 383–396.
34. D. Kim et al.: Metals, 10(3), 3, 2020, 410. https://doi.org/10.3390/met10030410.
35. R. Branco et al.: Metals, 8(1), 2018, 32. https://doi.org/10.3390/met8010032.
36. P. Petrousek, et al.: Acta Metallurgica Slovaca, 25(4), 2019, 283-290. https://doi.org/10.12776/ams.v25i4.1366.
37. A. Di Schino, P. Fogarait, D. Corapi, O. Di Pietro, C. Zitelli: Acta Metallurgica Slovaca, 26(1), 2020, 24-26. https://doi.org/10.36547/ams.26.1.329.
38. J. Bidulská, R. Bidulský, M.A. Grande, T. Kvačkaj: Materials, 12(22), 2019, 3724. https://doi.org/10.3390/ma12223724.
39. S. Yin et al.: Additive Manufacturing, 22, 2018, 592–600. https://doi.org/10.1016/j.addma.2018.06.005.
40. A. G. Demir, B. Previtali: International Journal of Advanced Manufacturing Technology, 93(5-8), 2017, 2697–2709. https://doi.org/10.1007/s00170-017-0697-z.
41. C. Tan, K. Zhou, W. Ma, P. Zhang, M. Liu, T. Kuang: Materials and Design, 134, 2017, 23–34. https://doi.org/10.1016/j.matdes.2017.08.026.
42. G. Casalino, S. L. Campanelli, N. Contuzzi, A. D. Ludovico: Optics and Laser Technology, 65, 2015, 151–58. https://doi.org/10.1016/j.optlastec.2014.07.021.
43. K. J. A. Brookes: Metal Powder Report, 71(3), 2016, 149–152. https://doi.org/10.1016/j.mprp.2016.04.087.
44. K. Kempen, E. Yasa, L. Thijs, J. P. Kruth, J. Van Humbeeck: Physics Procedia, 12, 2011, 255–263. https://doi.org/10.1016/j.phpro.2011.03.033.
45. J. Suryawanshi, K. G. Prashanth, U. Ramamurty: Journal of Alloys and Compounds 725, 2017, 355–64. https://doi.org/10.1016/j.jallcom.2017.07.177.
46. U. K. Viswanathan, G. K. Dey, V. Sethumadhavan: Materials Science and Engineering A, 398(1-2), 2005, 367-373. https://doi.org/10.1016/j.msea.2005.03.074.

DOI: 10.36547/ams.27.1.973